Abstract of Paper Proposed for Presentation at

SciTech 2015

Kissimmee, FL

5–9 January, 2015

Simulation of Atmospheric-Entry Capsules in the Subsonic Regime

Scott M. Murman, Robert E. Childs*, and Joseph A. Garcia

NASA Ames Research Center, Moffett Field, CA, USA

1 Introduction

Accurate prediction of the aerodynamic loads on atmospheric-entry capsules is still a challenge for Computational Fluid Dynamics (CFD) due to the three-dimensional separation and unsteady wake flow. At high supersonic speeds the combination of high dynamic pressures and suppression of some of the wake unsteadiness makes the problem tractable, and consistent predictions with common engineering Reynolds-averaged Navier-Stokes (RANS) models is often possible. When peak dynamic pressure is passed during the entry profile and the capsule enters the transonic and subsonic regimes, the unsteady wake "opens up" and errors in turbulence modeling can have a much greater impact on the prediction of aerodynamic performance. Unfortunately, this is often where greatest accuracy is required for Earth-entry systems, as there is little margin in control authority and complex parachute decelerator staging must be accomplished for targeted landing. Within NASA, the Orion

*Science and Technology Corporation

Figure 1: Artists rendition of the Orion Multi-Purpose Crew Vehicle.

Multi-Purpose Crew Vehicle project (*cf.* Fig. 1) is studying the requirements for consistent aerodynamic predictions using current "production" engineering CFD solvers and turbulence models. Simulations of the Orion vehicle for human exploration are further complicated by the existence of a rough ablated heatshield during normal mission profiles, and a smooth heatshield during abort scenarios. As will be shown, these two heatshield surfaces produce strongly differing aerodynamic environments.

The proposed paper details current "best practices" in prediction of aerodynamic loads for the Orion capsule in the subsonic regime, in comparison to recent experimental data[1–3]. This work utilizes the OVERFLOW solver[4], and examines numerical methods, mesh resolution, and turbulence modeling, including the effects of both transition and rough-wall models on the attached capsule heatshield boundary layer. The comparisons against experimental data include integrated loads, surface pressure distributions (both through pressure taps and pressure-sensitive paint), boundary-layer profiles, and Particle Image Velocimetry (PIV) measurements of the extended wake flowfield. A companion paper is being submitted to investigate similar issues using the OpenFOAM solver[5].

The current abstract briefly reviews the numerical methods being utilized, and presents an overview of the results computed to date. After this, the future work proposed for inclusion in the final paper is discussed.

2 Numerical Methods

The majority of the current work uses a simplified capsule model developed for public release in the experimental program of [3](*cf.* Fig. 2). While the capsule is a straightforward axisymmetric shape, the inclusion of the strut support adds significant geometric complication. Further, the actual Orion capsule geometry includes cutouts, windows, reaction-control surfaces, *etc.* which make the geometry definition more complex. In order to accommodate these complex geometries, while still maintaining computational efficiency, a structured overset grid system is utilized with the OVERFLOW solver. The overset grid system corresponding to the wind tunnel configuration of Fig. 2 is shown in Fig. 3. This system has 42M grid points as a baseline and can be further adapted using the OVERFLOW solver[6, 7].

The current work investigates two choices for numerical scheme: the (default) central differencing of the convective and acoustic terms, and the upwind HLLC flux in a MUSCL implementation. The upwind flux is often preferred for capsule aerodynamic database development due to the improved performance (robustness, shock-capturing) for high-speed flows, and the desire to maintain a single scheme for all database computations, as in [8]. The central-differencing schemes are often preferred for low-speed separated flows due to their lower numerical dissipation, especially when higher-order schemes are utilized. These two methods will be compared and contrasted in the full paper. The current abstract presents results using the HLLC upwind scheme.

There are three main turbulence models currently supported by OVERFLOW: the Spalart-Allmaras model[9], Wilcox's k-ω model[10], and Menter's Shear-Stress-Transport (SST) model[11]. From experience in the Orion project, the SST model has provided the most consistent predictions for capsule flowfields (*cf.* Chaderjian and Olsen[12], Stremel *et al.* [13] for an overview of the issues), and is the baseline model utilized in this work. Given this modeling framework, several augmentations are available. In the current work we investigate the use of hybrid-RANS/Detached-eddy Simulations (DES) to accurately capture the unsteady wake, transition modeling to predict the heatshield boundary at low-Reynolds-number wind-tunnel conditions, and roughness modeling to predict the ablated heatshield boundary layer.

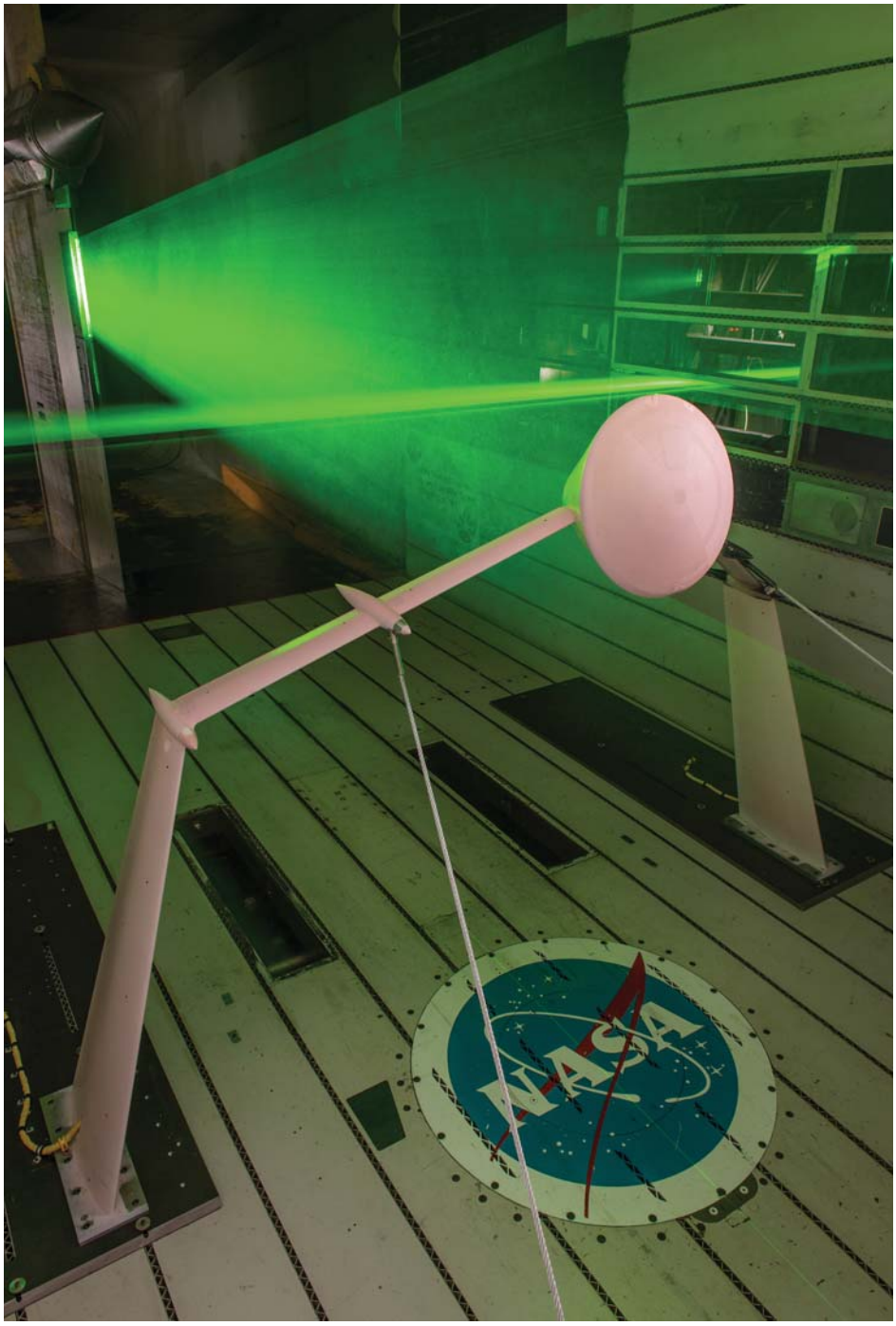

Figure 2: Capsule and strut configuration in the NASA Ames 11 ft. transonic wind tunnel[3]. The model is coated with PSP and the horizontal and vertical laser sheets cover the wake PIV planes.

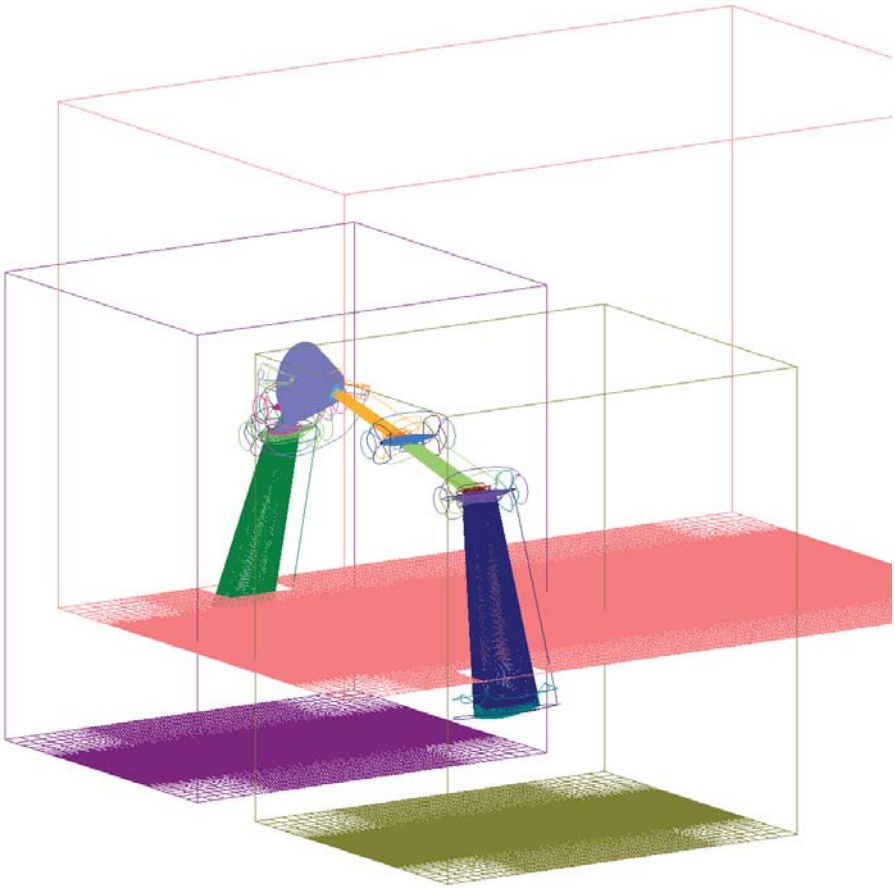

Figure 3: Overset grid system for the capsule and strut configuration in the NASA Ames 11 ft. transonic wind tunnel[3].

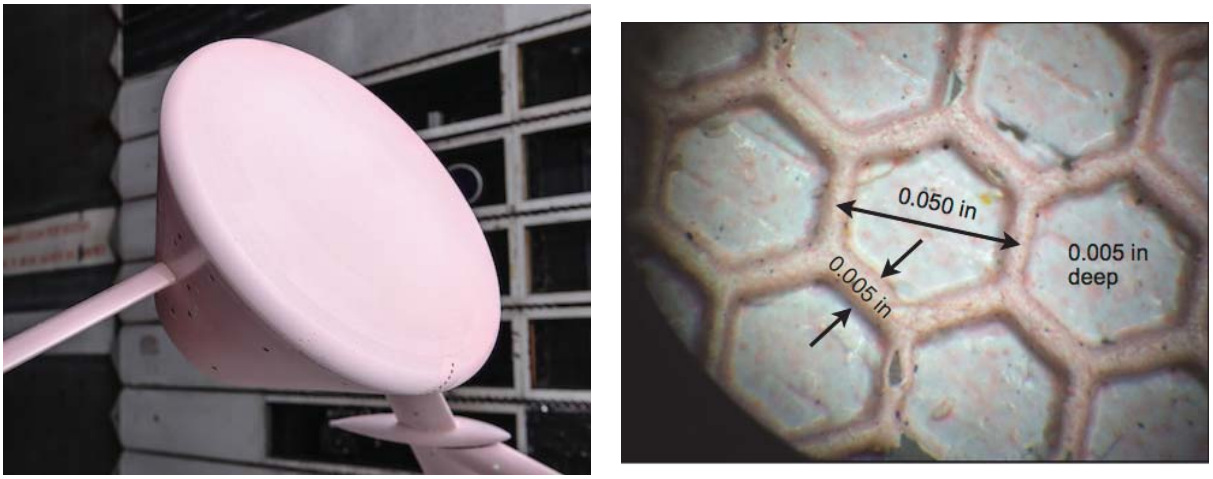

Figure 4: Hexagonal roughness from the experimental model in [3].

3 Wall Roughness

The AVCOAT honeycomb, which is the current Orion capsule heatshield design, ablates to a hexagonal roughness pattern. This roughness pattern scaled to the experimental capsule heatshield from [3] is shown in Fig. 4. OVERFLOW does not contain a standard wall roughness model. The roughness model of Knopp *et al.* [14] was implemented in OVERFLOW and verified using flat-plate boundary layer simulations. This model uses an equivalent sand-grain approach which does not accurately capture the boundary layer response to discrete roughness elements, as we have on the capsule heatshield. It is necessary to empirically calibrate the model for discrete roughness, which is done here using a multiplicative scale factor applied to the true roughness height. The model is calibrated at $M_\infty = 0.7$, $\alpha = 30^\circ$ against boundary layer profiles from [3], and then this calibration is tested against other available experimental conditions. Figure 5 shows the experimental and computational boundary layer profiles on the heatshield at $M_\infty = 0.7$, $\alpha = 30^\circ$. Discrete roughness scaling factors of $k_{SF} = 1$, 2, and 5 are tested, with a value of $k_{SF} = 2$ providing a good fit for the rough-wall profile. This value of $k_{SF} = 2$ is found to be a good fit at other flow conditions as well (Fig. 6), and all rough wall simulations presented herein use this scaling factor.

4 Surface Pressure Predictions

Figure 7 presents the computed surface pressure coefficient on the experimental model for a smooth and rough wall approximation. The presence of roughness reduces the "suc-

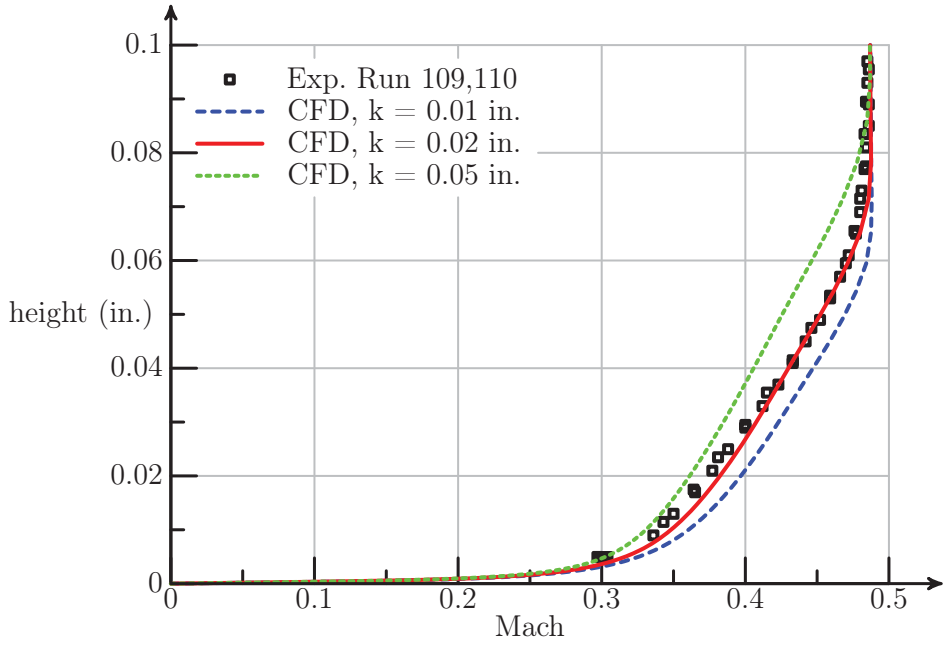

Figure 5: Calibration of the discrete roughness scale factor to the capsule heatshield boundary layer. The experimental roughness height is 0.01 in. Experimental data taken from [3].

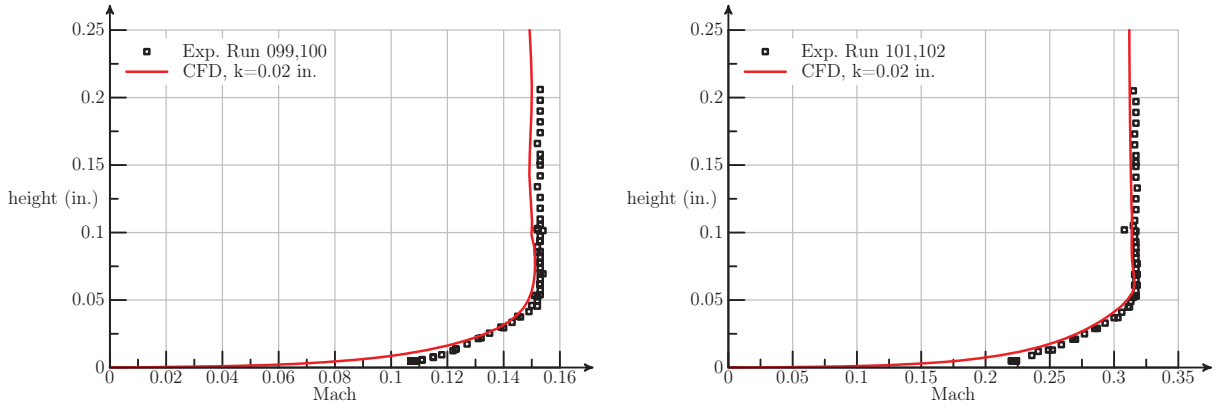

(a) $M_\infty = 0.3$, $\alpha = 15°$ **(b)** $M_\infty = 0.7$, $\alpha = 15°$

Figure 6: Test of the calibrated discrete roughness scale factor $k_{SF} = 2$. The experimental roughness height is 0.01 in. Experimental data taken from [3].

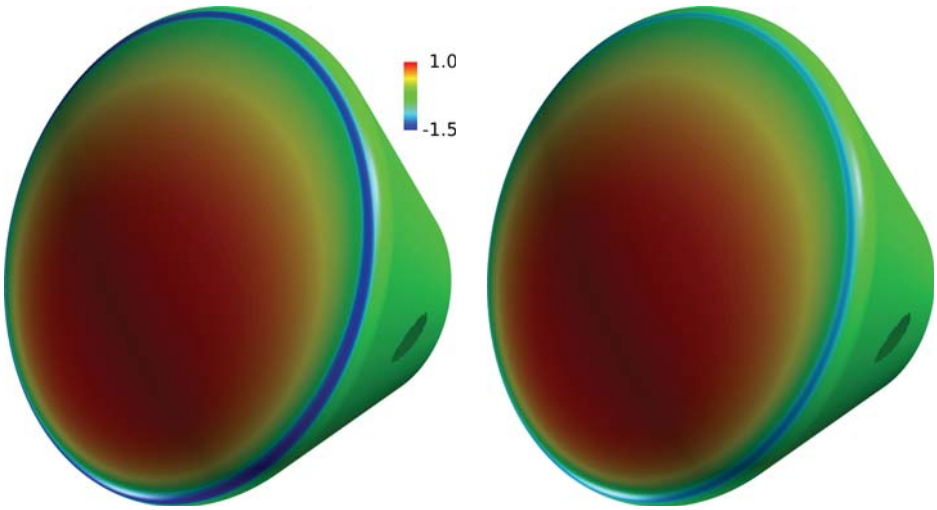

(a) smooth **(b)** rough

Figure 7: Computed distribution of surface pressure coefficient $M_\infty = 0.5$, $\alpha = 14°$, $Re_D = 8.7$M.

tion peak" near the heatshield shoulder associated with the attached boundary layer just upstream of separation from the surface by over 25% at these conditions. This is consistent with experimental observations, and is the motivation for including this roughness effect in the current computational approach.

Simulations of the experimental configuration using RANS and DES simulations were performed using the rough wall model. The unsteady DES simulations are time averaged after reaching a stationary state. The difference between the computed surface pressure and the pressure measured by the experimental pressure-sensitive paint (PSP) system is presented in Fig. 8. On the windward side of the capsule, the major discrepancy occurs near the suction peak and separation region for both simulations. The location of the experimental Kulite unsteady pressure transducers is visible from the increase in error at the 12, 1, and 3 o'clock positions. The region surrounding the Kulite installation is smooth in the experiment, and this local change is not modeled in the computations. As expected, for the attached boundary layer on the heatshield both RANS and DES simulations are essentially identical. The largest difference in the simulations occurs in the aft base region, where the RANS simulation overpredicts the pressure coefficient by roughly 30% of the freestream dynamic pressure, comparable to the magnitude of the difference near the suction peak. As we will see in the next section, the wake velocity in this region is also difficult for the RANS model to predict. The computed results consistently predict a delayed boundary-layer separation on the heatshield, and this error drives the error in the computed suction peak on the heatshield.

	PSP	RANS	DES
C_D	0.93	0.82	0.85
C_L	0.03	0.023	0.019

Table 1: Computed aerodynamic loads. $M_\infty = 0.5$, $\alpha = 14°$, $Re_D = 8.7$M.

Table 1 provides the computed lift and drag compared with the integrated PSP value. As expected, the numerical results under-predict the drag by roughly 10%. The final paper will include a detailed assessment of improvement strategies, including zonal turbulence modeling and rotation and curvature corrections.

5 Wake Velocity Predictions

The rough wall RANS and DES simulations outlined in the previous section are compared to the PIV wake velocity measurements in Fig. 9. Qualitatively, the computations are in relatively good agreement with the measurements, with the shear layer and reversed flow wake clearly visible. To highlight the differences, the CFD predictions are subtracted from the PIV measurements (Fig. 10). This shows relatively large error in the RANS far wake prediction, and in the prediction of the location of the separated shear layer for both simulations. This is expected from the discrepancy in boundary layer separation location highlighted in the previous section. The RANS near wake also contains a relatively large error near the aft body of the capsule, consistent with the difference in surface pressure from Fig. 8. Wake mesh refinement studies have been performed for these cases, and the results will be included in the final paper.

6 Future Work

The final paper will include a further mesh resolution study, and a comparison of mesh requirements for central difference and the HLLC upwind scheme, in terms of prediction of the capsule heatshield boundary layer separation and wake predictions. Further, turbulence modeling approaches will be examined, including rotation and curvature corrections, and transition modeling to predict lower Reynolds number smooth wall experimental data.

Acknowledgments

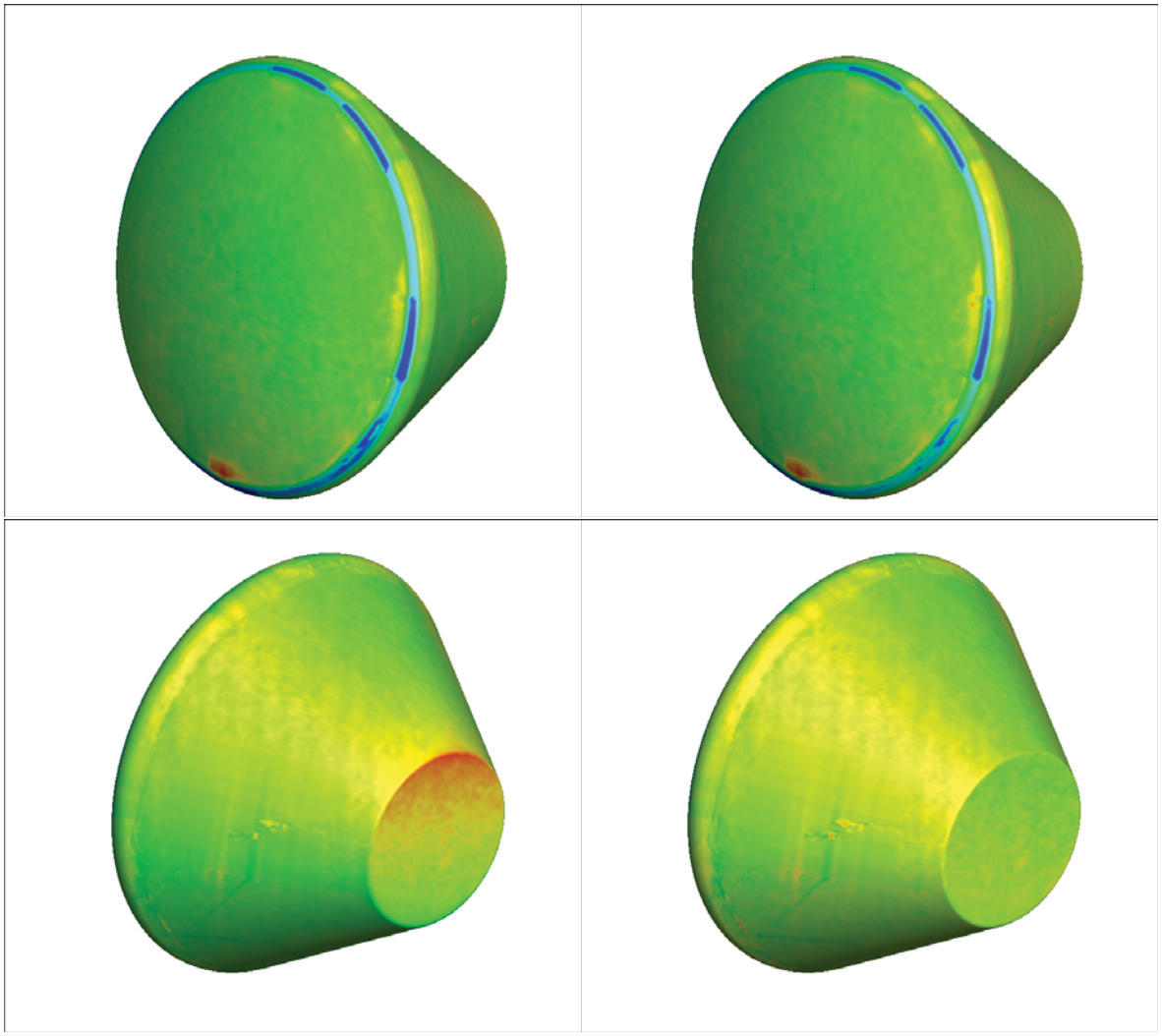

(c) RANS **(d)** DES

Figure 8: Difference in the surface pressure coefficient between simulation and PSP measurement (CFD-PSP). The limits of the difference are $\pm 0.3 q_\infty$, with green representing zero difference. $M_\infty = 0.5$, $\alpha = 14°$, $Re_D = 8.7$M.

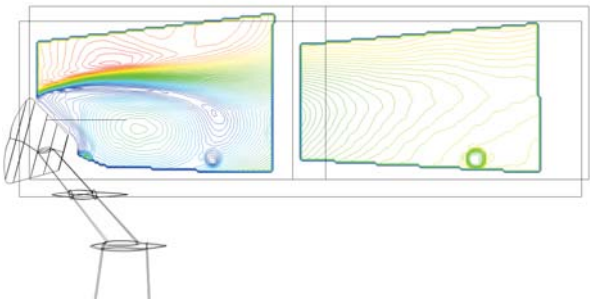

(a) PIV

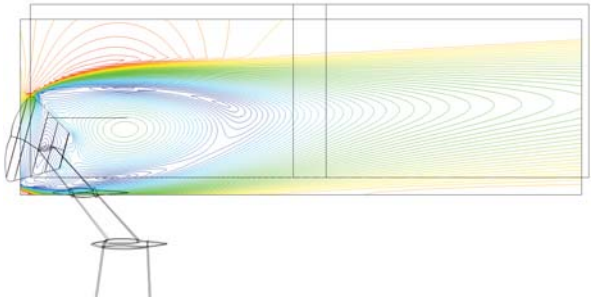

(b) RANS

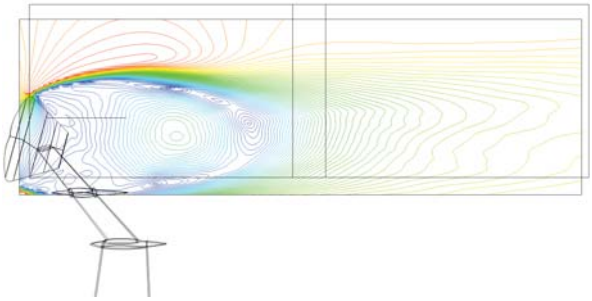

(c) DES

Figure 9: Measured and computed velocity magnitude in the wake. $M_\infty = 0.5$, $\alpha = 14°$, $Re_D = 8.7$M. Experimental data taken from [3].

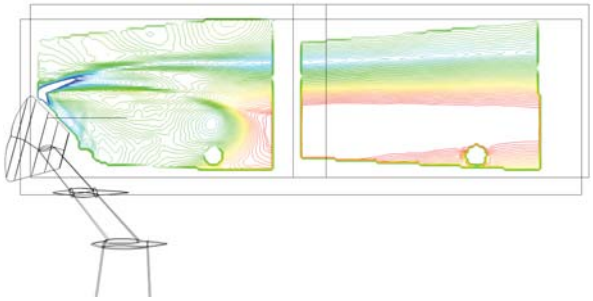

(a) RANS

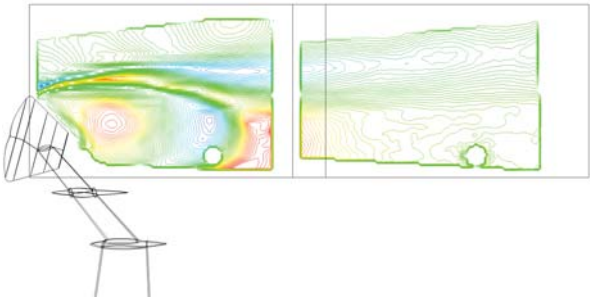

(b) DES

Figure 10: Difference in the wake velocity magnitude between simulation and PIV measurement (PIV-CFD). The limits of the difference are $\pm 0.25 M_\infty$. $M_\infty = 0.5$, $\alpha = 14°$, $Re_D = 8.7$M.

Dr. Stuart Rogers of NASA Ames Research Center provided the grid system for the experimental capsule configuration.

References

[1] Murphy, K.J., Bibb, K.L., Brauckmann, G.J., Rhode, M.N., Owens, B., Chan, D.T., Walker, E.L., Bell, J.H., and Wilson, T.M., "Orion Crew Module Aerodynamic Testing," AIAA Paper 2011-3502, 2011.

[2] Brauckmann, G., Chan, D., and Walker, E., "Final Report for Test 89-CA: High-Reynolds Number Test of the Orion Crew Module in the NASA LaRC National Transonic Facility," Tech. Rep. EG-CAP-12-65, MPCV Aerosciences, 2012.

[3] Ross, J.C., Heineck, J.T., Halcomb, N., Yamauchi, G.K., Garbeff, T., Burnside, N.T., Kushner, L.K., and Sellers, M., "Comprehensive Study of the Flow Around a Simplified Orion Capsule Model," AIAA Paper 2013-2815, 2013.

[4] Nichols, R.H., Tramel, R.W., and Buning, P.G., "Solver and Turbulence Model Upgrades to OVERFLOW 2 for Unsteady and High-Speed Applications," AIAA Paper 2006-2824, 2006.

[5] Nikaido, B.E., Murman, S.M., and Garcia, J.A., "OpenFOAM Simulations of Compressible High Reynolds Number External Aerodynamics," submitted to AIAA SciTech 2015.

[6] Buning, P.G. and Pulliam, T.H., "Cartesian Off-body Grid Adaptation for Viscous Time-Accurate Flow Simulation," AIAA Paper 2011-3693, 2011.

[7] Buning, P.G. and Pulliam, T.H., "Initial Implementation of Near-Body Grid Adaptation in OVERFLOW," in *11th Symposium on Overset Composite Grid and Solution Technology*, 2012.

[8] Childs, R.E., Garcia, J.A., Melton, J.E., Rogers, S.E., Shestopalov, A.J., and Vicker, D.J., "Overflow Simulation Guidelines for Orion Launch Abort Vehicle Aerodynamic Analyses," AIAA Paper 2011-3163, June 2011.

[9] Spalart, P.R. and Allmaras, S.R., "A one-equation turbulence model for aerodynamics flows," *La Recherche Aérospatiale*, vol. 1, pp. 5–21, 1994.

[10] Wilcox, D.C., "Formulation of the k-ω Turbulence Model Revisited," AIAA Paper 2007-1408, January 2007.

[11] Menter, F.R., "Two-Equation Eddy-Viscosity Turbulence Models for Engineering Applications," *AIAA Journal*, vol. 32, no. 8, pp. 1598–1605, 1994.

[12] Chaderjian, N.M. and Olsen, M.E, "Grid Resolution and Turbulence Model Effects on Space Capsule Navier-Stokes Simulations," AIAA Paper 2007-4562, June 2007.

[13] Stremel, P.M., McMullen, M.S., and Garcia, J.A., "Computational Aerodynamic Simulations of the Orion Crew Module," AIAA Paper 2011-3503, 2011.

[14] Knopp, T., Eisfeld, B., and Calvo, J.B., "A new extension for $k-\omega$ turbulence models to account for wall roughness," *International Journal of Heat and Fluid Flow*, vol. 30, pp. 54–65, 2009.